PERGAMON

International Journal of Solids and Structures 39 (2002) 5767–5785

INTERNATIONAL JOURNAL OF SOLIDS and STRUCTURES

www.elsevier.com/locate/ijsolstr

Singularity analysis of near-tip fields for notches formed from several anisotropic plates under bending

Jia Li *

Laboratoire d'Etudes et de Recherches en Mécanique des Structures, Blaise Pascal University of Clermont-Ferrand, Avenue Aristide Briand, 03100 Montluçon, France

Received 30 October 2001

Abstract

In this paper, we dealt with the problems concerning the singularities in the vicinity of a notch tip, or a crack tip as its special case, formed from several anisotropic plates subjected to bending and shearing forces. Attention was focused on the near-tip asymptotic analysis in monoclinic materials, which can be considered as the most general anisotropy in plate structures. The Reissner assumptions of the plate theory were adopted. First, the fundamental equations for a monoclinic plate were established in the cylindrical coordinate system by means of the Hellinger–Reissner variational principle. Second, by introducing the suitable dual variable vectors, the governing equations were established in the frame of the Hamiltonian system. These governing equations are particularly efficient to deal with multi-material problems because all variables used are continuous across the interfaces. Third, a simple but highly accurate numerical algorithm was proposed to resolve the governing equations. Finally, several numerical examples have been given in order to test the efficiency and the simplicity of the present theory in studying the asymptotic fields in the vicinity of a notch tip formed from several anisotropic plates.

Keywords: Crack; Notch; Plate; Asymptotic analysis; Anisotropy; Near-tip field; Singularity; Bending

1. Introduction

Stress concentration in thin plates with cracks has been a subject of numerous researches for several decades due to its importance in analysis of thin-wall structures such as aircraft fuselages. The principal theories studying the asymptotic fields near a crack tip in a plate loaded by bending forces were established in the 1960s of the precedent century (Williams, 1961; Sih et al., 1962; Knowels and Wang, 1960; Hartranft and Sih, 1968, etc.). More detailed analyses have been added into these theories later (Delale and Erdogan, 1979; Murthy et al., 1981; Boduroglu and Erdogan, 1983; Sosa and Eischen, 1986; Hui and Zehnder, 1993; Young and Sun, 1993; Su and Leung, 2001, etc.). In these analyses, two plate theories, the Poisson–Kirchhoff theory and the Mindlin–Reissner theory were essentially followed. The Poisson–Kirchhoff theory

* Fax: +33-4-70-02-20-78.
E-mail address: lijia@moniut.univ-bpclermont.fr (J. Li).

0020-7683/02/$ - see front matter
PII: S0020-7683(02)00406-7

provides rather simple mathematical solutions, but gives some physically incorrect behaviors about the near-tip fields. In fact, according to this theory, for cracks in homogeneous elastic plates, the transverse shear stresses vary asymptotically as $r^{-3/2}$ instead of $r^{-1/2}$ as r tends to zero. On the other hand, Reissner's thin plate theory gives physically more reasonable results, but the solution of the six-order differential equations remains difficult for many problems posed.

The next studies were carried out in determining the near-tip fields of a crack lying along or normally touching the interface of a bimaterial plate. Sih and Rice (1964) have applied the Poisson–Kirchhoff theory and solved the bimaterial plate problem with an interface crack. The Riemann–Hilbert formulation was later given by Sih (1962). The Kirchhoff theory has also been used to solve the bimaterial plate problem with a crack normally touching the interface (Sih and Chen, 1981).

Anisotropy is a very important property in composite plates. The crack-tip fields in anisotropic plates have been first studied by Ang and Williams (1961), who presented a closed form solution for an orthotropic, infinite plate having a finite crack within the context of the Kirchhoff theory. Using the similar concept, Sih and Chen (1981) further extended to an anisotropic plate using the Lekhnitskii formalism. Recently, Yuan and Yang (2000) studied the same problem by applying the Reissner plate theory and the Stroh formalism.

It is obvious that problems with cracks or notches in anisotropic plates have not been thoroughly studied yet, especially when the cracks or notches are formed from two or more anisotropic plates. In fact, these configurations can be found in many engineering structures such like the welded structures, composites and so on. In this paper, we propose to find out asymptotic fields near a notch tip formed by several monoclinic thin plates subjected to bending and transverse shearing forces. This is a more general situation in this kind of structures. The corresponding crack problems or bimaterial problems can be treated as its special cases. The existing traditional theories dealing with the anisotropic materials are quite fastidious in solving the posed problem. In this work, we will use a new methodology proposed by Zhong (1995) which consists in introducing Hamiltonian system, which is usually studied in rational mechanics, into continuum mechanics. By choosing appropriate dual variables in the state space, we have established the governing equations on the basis of the Reissner plate theory. We also proposed a simple but highly accurate numerical method to solve the governing equations. Finally, we selected a few examples, some of them have been solved in the literature, and others not yet. These examples were solved by means of the present method in order to test its accuracy and its potential possibilities for further applications.

2. Governing equations of the problem

Let us consider a monoclinic plate subjected to bending. In fact, the general anisotropy is rather rare in plate-based structures. The composite plates use to present at least one symmetrical plane parallel to the mid-plane, this leads to a monoclinic system in the most general case.

Let us attach to a plate a cylindrical coordinate system (r, θ, z) and a Cartesian coordinate system $(x = r\cos\theta, y = r\sin\theta, z)$. The r–θ or x–y plane corresponds to the mid-plane of the plate. We first write the stress components in the Cartesian coordinate system and in the cylindrical coordinate system as $\boldsymbol{\sigma}_{xyz} = \{\sigma_x \quad \sigma_y \quad \sigma_z \quad \sigma_{xy} \quad \sigma_{xz} \quad \sigma_{yz}\}^{\mathrm{T}}$ and $\boldsymbol{\sigma}_{r\theta z} = \{\sigma_r \quad \sigma_\theta \quad \sigma_z \quad \sigma_{r\theta} \quad \sigma_{rz} \quad \sigma_{\theta z}\}^{\mathrm{T}}$ respectively. The corresponding strain components are $\boldsymbol{\varepsilon}_{xyz} = \{\varepsilon_x \quad \varepsilon_y \quad \varepsilon_z \quad \gamma_{xy} \quad \gamma_{xz} \quad \gamma_{yz}\}^{\mathrm{T}}$ and $\boldsymbol{\varepsilon}_{r\theta z} = \{\varepsilon_r \quad \varepsilon_\theta \quad \varepsilon_z \quad \gamma_{r\theta} \quad \gamma_{rz} \quad \gamma_{\theta z}\}^{\mathrm{T}}$ respectively. One can write the strain–stress relationship for an elastic monoclinic material in the Cartesian coordinate system, as follows:

$$\boldsymbol{\varepsilon}_{xyz} = \boldsymbol{S}_{xyz}\boldsymbol{\sigma}_{xyz} \tag{1}$$

$\boldsymbol{S}_{xyz}$ is the compliance matrix of the material, namely:

$$\boldsymbol{S}_{xyz} = \begin{bmatrix} s_{11} & s_{12} & s_{13} & s_{14} & 0 & 0 \\ s_{21} & s_{22} & s_{23} & s_{24} & 0 & 0 \\ s_{31} & s_{32} & s_{33} & s_{34} & 0 & 0 \\ s_{41} & s_{42} & s_{44} & s_{44} & 0 & 0 \\ 0 & 0 & 0 & 0 & s_{55} & s_{56} \\ 0 & 0 & 0 & 0 & s_{65} & s_{66} \end{bmatrix} \tag{2}$$

$s_{ij}(i,j=1,6)$ are the elastic compliances. In the cylindrical system, the stress and strain components can be obtained from their corresponding quantities in the Cartesian system with a coordinate rotation, namely:

$$\boldsymbol{\sigma}_{r\theta z} = \boldsymbol{T}_{\sigma}\boldsymbol{\sigma}_{xyz} \quad \boldsymbol{\varepsilon}_{r\theta z} = \boldsymbol{T}_{\varepsilon}\boldsymbol{\varepsilon}_{xyz} \tag{3}$$

Therefore, the stress–strain relationship in the cylindrical system is:

$$\boldsymbol{\varepsilon}_{r\theta z} = \boldsymbol{S}_{r\theta z}\boldsymbol{\sigma}_{r\theta z}$$

with

$$\boldsymbol{S}_{r\theta z} = \boldsymbol{T}_{\varepsilon}\boldsymbol{S}_{xyz}\boldsymbol{T}_{\sigma}^{-1} \tag{4}$$

where

$$\boldsymbol{T}_{\sigma} = \begin{bmatrix} \cos^2\theta & \sin^2\theta & 0 & 2\cos\theta\sin\theta & 0 & 0 \\ \sin^2\theta & \cos^2\theta & 0 & -2\cos\theta\sin\theta & 0 & 0 \\ 0 & 0 & 1 & 0 & 0 & 0 \\ -\cos\theta\sin\theta & \cos\theta\sin\theta & 0 & \cos^2\theta-\sin^2\theta & 0 & 0 \\ 0 & 0 & 0 & 0 & \cos\theta & \sin\theta \\ 0 & 0 & 0 & 0 & -\sin\theta & \cos\theta \end{bmatrix}$$

$$\boldsymbol{T}_{\varepsilon} = \begin{bmatrix} \cos^2\theta & \sin^2\theta & 0 & \cos\theta\sin\theta & 0 & 0 \\ \sin^2\theta & \cos^2\theta & 0 & -\cos\theta\sin\theta & 0 & 0 \\ 0 & 0 & 1 & 0 & 0 & 0 \\ -2\cos\theta\sin\theta & 2\cos\theta\sin\theta & 0 & \cos^2\theta-\sin^2\theta & 0 & 0 \\ 0 & 0 & 0 & 0 & \cos\theta & \sin\theta \\ 0 & 0 & 0 & 0 & -\sin\theta & \cos\theta \end{bmatrix} \tag{5}$$

Eq. (4) shows that in the cylindrical system, the compliance matrix is not a constant matrix but function of θ. Nevertheless, the compliance matrix $\boldsymbol{S}_{r\theta z}$ keeps always the same mathematical structure as $\boldsymbol{S}_{xyz}$, i.e., $\boldsymbol{S}_{r\theta z} = \begin{bmatrix} \boldsymbol{S}_{44} & \boldsymbol{0} \\ \boldsymbol{0} & \boldsymbol{S}_{22} \end{bmatrix}$, where $\boldsymbol{S}_{44}$ is a 4×4 symmetrical matrix and $\boldsymbol{S}_{22}$ is a 2×2 symmetrical matrix. Hereafter we work exclusively in the cylindrical system, therefore the subscript $_{r\theta z}$ will be omitted in order to simplify the notations.

In the cylindrical coordinate system, the conventional notations are used in this paper to describe the mechanical quantities in a plate, see Fig. 1:

Displacement components: $\{u_r \quad u_\theta \quad w\}$;
Rotation components: $\{\tilde{\boldsymbol{u}}_r \quad \tilde{\boldsymbol{u}}_\theta\}$;
Bending moments: $\{M_{rr} \quad M_{\theta\theta} \quad M_{r\theta}\}$;
Shear forces: $\{Q_{rz} \quad Q_{\theta z}\}$.

The main assumptions of the Mindlin–Reissner theory state that the in-plane displacements u_r and u_θ vary linearly through the thickness and that the displacement w is independent of z, i.e.,

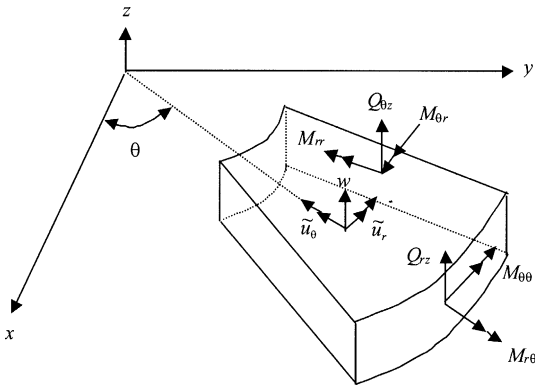

Fig. 1. Internal forces and displacement components.

$$u_r = z\tilde{u}_r(r,\theta) \quad u_\theta = z\tilde{u}_\theta(r,\theta) \quad w = w(r,\theta) \tag{6}$$

where $\tilde{u}_r$ and $\tilde{u}_\theta$ are functions independent of the z-coordinate.

The boundary conditions on the both sides of the plate are prescribed as follows:

$$\begin{aligned} &\sigma_{zz} = -q \quad \sigma_{rz} = \sigma_{\theta z} = 0 \quad \text{on } z = h/2 \\ &\sigma_{zz} = 0 \quad \sigma_{rz} = \sigma_{\theta z} = 0 \quad \text{on } z = -h/2 \end{aligned} \tag{7}$$

where q is the normal pressure applied on the plate surface and h is the thickness of the plate.

According to the plate theory, we assume the following relationships between the stress components and the internal force components:

$$\begin{aligned} &\sigma_{rr} = \frac{12z}{h^3}M_{rr} \quad \sigma_{\theta\theta} = \frac{12z}{h^3}M_{\theta\theta} \quad \sigma_{r\theta} = \frac{12z}{h^3}M_{r\theta} \\ &\sigma_{rz} = \frac{3}{2h}\left(1 - \frac{4z^2}{h^2}\right)Q_{rz} \quad \sigma_{\theta z} = \frac{3}{2h}\left(1 - \frac{4z^2}{h^2}\right)Q_{\theta z} \quad \sigma_{zz} = -q\frac{3}{4}\left(2\frac{z}{h} - \frac{8}{3}\frac{z^3}{h^3} + \frac{2}{3}\right) \end{aligned} \tag{8}$$

In order to solve the problem more easily, we perform the following variable changes:

$$\begin{aligned} &r = \mathrm{e}^{\xi} \\ &M_{rr} = \frac{\widetilde{M}_{rr}}{r} \quad M_{\theta\theta} = \frac{\widetilde{M}_{\theta\theta}}{r} \quad M_{r\theta} = \frac{\widetilde{M}_{r\theta}}{r} \\ &w = r\tilde{w} \end{aligned} \tag{9}$$

The functional of the Hellinger–Reissner principle is defined as follows:

$$\delta\left\{\int_V \left[\boldsymbol{\sigma}^{\mathrm{T}}\boldsymbol{E}^{\mathrm{T}}(\nabla)\boldsymbol{u} - \boldsymbol{f}^{\mathrm{T}}\boldsymbol{u} - U^*(\sigma)\right]\mathrm{d}V - \int_{S_\sigma}(\boldsymbol{X}_{\boldsymbol{n}}^{\mathrm{T}} - \overline{\boldsymbol{X}}_{\boldsymbol{n}}^{\mathrm{T}})\boldsymbol{u}\,\mathrm{d}S - \int_{S_u}\boldsymbol{X}_n^{\mathrm{T}}\overline{\boldsymbol{u}}\,\mathrm{d}S\right\} = 0 \tag{10}$$

where V is the volume of the plate; $\boldsymbol{f}$ is the body force vector, $\boldsymbol{f}=\boldsymbol{0}$ is considered in this work; $\boldsymbol{E}(\nabla)$ is a differential operator, $\boldsymbol{\varepsilon} = \boldsymbol{E}^{\mathrm{T}}(\nabla)\boldsymbol{u}$; U^* is referred to as the complementary energy density; $\boldsymbol{u} = \overline{\boldsymbol{u}}$ on S_u and $\boldsymbol{X}_n = \overline{\boldsymbol{X}}_n$ on S_σ are the prescribed boundary conditions. By substituting (6) and (8) into (10), and by taking the variable changes (9) into account, we can rewrite the Hellinger–Reissner principle (10) as follows:

$$\delta\Bigg\{\int_{S_m}\Bigg[\frac{6}{h^3}\left(s_{11}\widetilde{M}_{rr}^2+s_{22}\widetilde{M}_{\theta\theta}^2+s_{44}\widetilde{M}_{r\theta}^2\right)+2\left(s_{12}\widetilde{M}_{rr}\widetilde{M}_{\theta\theta}+s_{14}\widetilde{M}_{rr}\widetilde{M}_{r\theta}+s_{24}\widetilde{M}_{\theta\theta}\widetilde{M}_{r\theta}\right)$$
$$-\mathrm{e}^{\xi}\frac{h^2q}{5}\left(s_{13}\widetilde{M}_{rr}+s_{23}\widetilde{M}_{\theta\theta}+s_{36}\widetilde{M}_{r\theta}\right)+\mathrm{e}^{2\xi}\frac{13h}{70}s_{33}q^2+\frac{\mathrm{e}^{2\xi}}{hk}\left(s_{55}Q_{rz}^2.+s_{66}Q_{\theta z}^2+2s_{56}Q_{rz}Q_{\theta z}\right)$$
$$+\left(\frac{\partial\widetilde{M}_{rr}}{\partial\xi}+\frac{\partial\widetilde{M}_{r\theta}}{\partial\theta}-\widetilde{M}_{\theta\theta}-\mathrm{e}^{2\xi}Q_{rz}\right)\tilde{u}_r+\left(\frac{\partial\widetilde{M}_{r\theta}}{\partial\xi}+\frac{\partial\widetilde{M}_{\theta\theta}}{\partial\theta}+\widetilde{M}_{r\theta}-\mathrm{e}^{2\xi}Q_{\theta z}\right)\tilde{u}_\theta$$
$$+\left(\frac{\partial Q_{rz}}{\partial\xi}+\frac{\partial Q_{\theta z}}{\partial\theta}+Q_{rz}+\mathrm{e}^{\xi}q\right)w\Bigg]\mathrm{d}\xi\,\mathrm{d}\theta-\int(\text{terms on boundaries})\,\mathrm{d}S\Bigg\}=0 \tag{11}$$

with S_m being the mid-plane of the plate. Perform now the variations with respect to $\widetilde{M}_{ij}$, Q_i and $\tilde{u}_i$. After some mathematical deductions, we can find the following fundamental equations:

Equilibrium equations:

$$\begin{aligned}
&\frac{\partial\widetilde{M}_{rr}}{\partial\xi}+\frac{\partial\widetilde{M}_{r\theta}}{\partial\theta}-\widetilde{M}_{\theta\theta}=\mathrm{e}^{2\xi}Q_{rz}\\
&\frac{\partial\widetilde{M}_{r\theta}}{\partial\xi}+\frac{\partial\widetilde{M}_{\theta\theta}}{\partial\theta}+\widetilde{M}_{r\theta}=\mathrm{e}^{2\xi}Q_{\theta z}\\
&\frac{\partial Q_{rz}}{\partial\xi}+\frac{\partial Q_{\theta z}}{\partial\theta}+Q_{rz}=-\mathrm{e}^{\xi}q
\end{aligned} \tag{12}$$

Relationships between the displacements and internal force components:

$$\begin{aligned}
&\begin{Bmatrix}\dfrac{\partial\tilde{u}_r}{\partial\xi}\\ \tilde{u}_r+\dfrac{\partial\tilde{u}_\theta}{\partial\theta}\\ \dfrac{\partial\tilde{u}_\theta}{\partial\xi}-\tilde{u}_\theta+\dfrac{\partial\tilde{u}_r}{\partial\theta}\end{Bmatrix}=\frac{12}{h^3}\begin{bmatrix}s_{11}&s_{12}&s_{14}\\ s_{21}&s_{22}&s_{24}\\ s_{41}&s_{42}&s_{44}\end{bmatrix}\begin{Bmatrix}\widetilde{M}_{rr}\\ \widetilde{M}_{\theta\theta}\\ \widetilde{M}_{r\theta}\end{Bmatrix}-\frac{\mathrm{e}^{\xi}q}{hk}\begin{Bmatrix}s_{13}\\ s_{23}\\ s_{34}\end{Bmatrix}\\
&\begin{Bmatrix}\tilde{u}_r+\tilde{w}+\dfrac{\partial\tilde{w}}{\partial\xi}\\ \tilde{u}_\theta+\dfrac{\partial\tilde{w}}{\partial\theta}\end{Bmatrix}=\frac{1}{hk}\begin{bmatrix}s_{55}&s_{56}\\ s_{65}&s_{66}\end{bmatrix}\begin{Bmatrix}Q_{rz}\\ Q_{\theta z}\end{Bmatrix}
\end{aligned} \tag{13}$$

In the case of the isotropic plate, the material coefficients s_{ij} are constants: $s_{11}=s_{22}=s_{33}=1/E$; $s_{12}=s_{23}=s_{13}=v/E$; $s_{44}=s_{55}=s_{66}=2(1+v)/E$ and $s_{14}=s_{24}=s_{34}=0$. In this case, the equilibrium equations remain identical to (12), while the relationships between the displacements and internal force components become:

$$\begin{aligned}
&\begin{Bmatrix}\dfrac{\partial\tilde{u}_r}{\partial\xi}\\ \tilde{u}_r+\dfrac{\partial\tilde{u}_\theta}{\partial\theta}\\ \dfrac{\partial\tilde{u}_\theta}{\partial\xi}-\tilde{u}_\theta+\dfrac{\partial\tilde{u}_r}{\partial\theta}\end{Bmatrix}=\frac{12}{Eh^3}\begin{bmatrix}1&-v&0\\ -v&1&0\\ 0&0&2(1+v)\end{bmatrix}\begin{Bmatrix}\widetilde{M}_{rr}\\ \widetilde{M}_{\theta\theta}\\ \widetilde{M}_{r\theta}\end{Bmatrix}-\frac{\mathrm{e}^{\xi}q}{Ehk}\begin{Bmatrix}-v\\ -v\\ 0\end{Bmatrix}\\
&\begin{Bmatrix}\tilde{u}_r+\tilde{w}+\dfrac{\partial\tilde{w}}{\partial\xi}\\ \tilde{u}_\theta+\dfrac{\partial\tilde{w}}{\partial\theta}\end{Bmatrix}=\frac{2(1+v)}{Ehk}\begin{Bmatrix}Q_{rz}\\ Q_{\theta z}\end{Bmatrix}
\end{aligned} \tag{14}$$

In order to establish the governing equations, we first eliminate the quantities $\widetilde{M}_{rr}$ and Q_{rz} from the fundamental equations. From the first and the forth equations of (13), we can write:

$$\begin{aligned}\widetilde{M}_{rr} &= \frac{1}{s_{11}}\left(\frac{h^3}{12}\frac{\partial u_r}{\partial \xi} + \mathrm{e}^{\xi}\frac{h^2 q}{10}s_{13}\right) - \frac{1}{s_{11}}\left(s_{12}\widetilde{M}_{\theta\theta} + s_{14}\widetilde{M}_{r\theta}\right)\\ Q_{rz} &= \frac{hk}{s_{55}}\left(\tilde{u}_r + \tilde{w} + \frac{\partial \tilde{w}}{\partial \xi}\right) - \frac{s_{56}}{s_{55}}Q_{\theta z}\end{aligned} \tag{15}$$

By substituting (15) into Eqs. (12) and (13) then by denoting $(\bullet) = \partial/\partial\theta$, we obtain:

$$\begin{aligned}\dot{\tilde{u}}_r &= \frac{s_{41}}{s_{11}}\frac{\partial \tilde{u}_r}{\partial \xi} + \left(1 - \frac{\partial}{\partial \xi}\right)\tilde{u}_\theta + \frac{12}{h^3}\left(s_{44} - \frac{s_{14}^2}{s_{11}}\right)\widetilde{M}_{r\theta} + \frac{12}{h^3}\left(s_{42} - \frac{s_{41}s_{12}}{s_{11}}\right)\widetilde{M}_{\theta\theta} - \frac{\mathrm{e}^{\xi} q}{hk}\left(s_{34} - \frac{s_{41}s_{13}}{s_{11}}\right)\\ \dot{\tilde{u}}_\theta &= \left(\frac{s_{12}}{s_{11}}\frac{\partial}{\partial \xi} - 1\right)\tilde{u}_r + \frac{12}{h^3}\left(s_{24} - \frac{s_{21}s_{14}}{s_{11}}\right)\widetilde{M}_{r\theta} + \frac{12}{h^3}\left(s_{22} - \frac{s_{12}^2}{s_{11}}\right)\widetilde{M}_{r\theta} - \frac{\mathrm{e}^{\xi} q}{hk}\left(s_{23} - \frac{s_{21}s_{13}}{s_{11}}\right)\\ \dot{\tilde{w}} &= \frac{s_{65}}{s_{55}}\tilde{u}_r - \tilde{u}_\theta + \frac{s_{65}}{s_{55}}\left(1 + \frac{\partial}{\partial \xi}\right)\tilde{w} + \frac{1}{hk}\left(s_{66} - \frac{s_{56}^2}{s_{55}}\right)Q_{\theta z}\\ \dot{\widetilde{M}}_{r\theta} &= -\frac{h^3}{12 s_{11}}\frac{\partial^2 \tilde{u}_r}{\partial \xi^2} + \frac{s_{14}}{s_{11}}\frac{\partial \widetilde{M}_{r\theta}}{\partial \xi} + \left(1 + \frac{s_{12}}{s_{11}}\frac{\partial}{\partial \xi}\right)\widetilde{M}_{\theta\theta} - \mathrm{e}^{\xi}\frac{h^2 q}{10}\frac{s_{13}}{s_{11}} + \mathrm{e}^{2\xi}\frac{hk}{s_{55}}\left(\tilde{u}_r + \tilde{w} + \frac{\partial \tilde{w}}{\partial \xi}\right) - \mathrm{e}^{2\xi}\frac{s_{56}}{s_{55}}Q_{\theta z}\\ \dot{\widetilde{M}}_{\theta\theta} &= -\left(1 + \frac{\partial}{\partial \xi}\right)\widetilde{M}_{r\theta} + \mathrm{e}^{2\xi}Q_{\theta z}\\ \dot{Q}_{\theta z} &= -\left(1 + \frac{\partial}{\partial \xi}\right)\left[\frac{hk}{s_{55}}\left(\tilde{u}_r + \tilde{w} + \frac{\partial \tilde{w}}{\partial \xi}\right) - \frac{s_{56}}{s_{55}}Q_{\theta z}\right] - \mathrm{e}^{\xi} q\end{aligned} \tag{16}$$

We define the following duals variables:

$$\begin{aligned}&\boldsymbol{q}_1 = \left\{\tilde{u}_r \quad \tilde{u}_\theta\right\}^{\mathrm{T}} \quad \boldsymbol{p}_1 = \left\{\widetilde{M}_{r\theta} \quad \widetilde{M}_{\theta\theta}\right\}^{\mathrm{T}}\\ &\boldsymbol{q}_2 = \tilde{w} \quad \boldsymbol{p}_2 = Q_{\theta z}\end{aligned} \tag{17}$$

and

$$\boldsymbol{v}_1 = \left\{\boldsymbol{q}_1^{\mathrm{T}} \quad \boldsymbol{p}_1^{\mathrm{T}}\right\}^{\mathrm{T}} \quad \boldsymbol{v}_2 = \left\{\boldsymbol{q}_2^{\mathrm{T}} \quad \boldsymbol{p}_2^{\mathrm{T}}\right\}^{\mathrm{T}} \tag{18}$$

Therefore, (16) can be rewritten as follows:

$$\begin{aligned}\dot{\boldsymbol{v}}_1 &= \boldsymbol{A}\boldsymbol{v}_1 + \mathrm{e}^{\xi}\boldsymbol{f}_1 + \mathrm{e}^{2\xi}\boldsymbol{D}\boldsymbol{v}_1 + \mathrm{e}^{2\xi}\boldsymbol{E}\boldsymbol{v}_2\\ \dot{\boldsymbol{v}}_2 &= \boldsymbol{B}\boldsymbol{v}_1 + \boldsymbol{C}\boldsymbol{v}_2 + \mathrm{e}^{\xi}\boldsymbol{f}_2\end{aligned} \tag{19}$$

with

$$\boldsymbol{A} = \begin{bmatrix} \dfrac{s_{41}}{s_{11}}\dfrac{\partial}{\partial \xi} & 1 - \dfrac{\partial}{\partial \xi} & \dfrac{12}{h^3}\left(s_{44} - \dfrac{s_{14}^2}{s_{11}}\right) & \dfrac{12}{h^3}\left(s_{42} - \dfrac{s_{41}s_{12}}{s_{11}}\right)\\ \dfrac{s_{12}}{s_{11}}\dfrac{\partial}{\partial \xi} - 1 & 0 & \dfrac{12}{h^3}\left(s_{24} - \dfrac{s_{21}s_{14}}{s_{11}}\right) & \dfrac{12}{h^3}\left(s_{22} - \dfrac{s_{12}^2}{s_{11}}\right)\\ -\dfrac{h^3}{12 s_{11}}\dfrac{\partial^2}{\partial \xi^2} & 0 & \dfrac{s_{14}}{s_{11}}\dfrac{\partial}{\partial \xi} & \dfrac{s_{12}}{s_{11}}\dfrac{\partial}{\partial \xi} + 1\\ 0 & 0 & -1 - \dfrac{\partial}{\partial \xi} & 0 \end{bmatrix}$$

$$\boldsymbol{C}=\begin{bmatrix} \frac{s_{65}}{s_{55}}\left(\frac{\partial}{\partial\xi}+1\right) & \frac{1}{hk}\left(s_{66}-\frac{s_{56}^2}{s_{55}}\right) \\ -\frac{hk}{s_{55}}\left(1+\frac{\partial}{\partial\xi}\right)^2 & \frac{s_{56}}{s_{55}}\left(\frac{\partial}{\partial\xi}+1\right) \end{bmatrix} \qquad \boldsymbol{B}=\begin{bmatrix} \frac{s_{65}}{s_{55}} & -1 & 0 & 0 \\ -\frac{hk}{s_{55}}\left(1+\frac{\partial}{\partial\xi}\right) & 0 & 0 & 0 \end{bmatrix}$$

$$\boldsymbol{D}=\frac{hk}{s_{55}}\begin{bmatrix} 0&0&0&0\\ 0&0&0&0\\ 0&1&0&0\\ 0&0&0&0 \end{bmatrix} \qquad \boldsymbol{E}=\begin{bmatrix} 0 & 0 \\ 0 & 0 \\ \frac{hk}{s_{55}}\left(1+\frac{\partial}{\partial\xi}\right) & -\frac{s_{65}}{s_{55}} \\ 0 & 1 \end{bmatrix} \qquad \boldsymbol{f}_1=q\begin{Bmatrix} \frac{1}{hk}\left(\frac{s_{41}s_{13}}{s_{11}}-s_{43}\right) \\ \frac{1}{hk}\left(\frac{s_{21}s_{13}}{s_{11}}-s_{23}\right) \\ -\frac{h^2}{10}\frac{s_{13}}{s_{11}} \\ 0 \end{Bmatrix}$$

$$\boldsymbol{f}_2=q\begin{Bmatrix} 0 \\ -1 \end{Bmatrix} \tag{20}$$

In the isotropic case, the governing differential equations are always written as (19) but with the following matrices:

$$\boldsymbol{A}=\begin{bmatrix} 0 & 1-\frac{\partial}{\partial\xi} & \frac{24(1+\nu)}{Eh^3} & 0 \\ -1-\nu\frac{\partial}{\partial\xi} & 0 & 0 & \frac{12(1-\nu^2)}{Eh^3} \\ -\frac{Eh^3}{12}\frac{\partial^2}{\partial\xi^2} & 0 & 0 & 1-\nu\frac{\partial}{\partial\xi} \\ 0 & 0 & -1-\frac{\partial}{\partial\xi} & 0 \end{bmatrix} \qquad \boldsymbol{C}=\begin{bmatrix} 0 & \frac{2(1+\nu)}{Ehk} \\ -\frac{Ehk}{2(1+\nu)}\left(1+\frac{\partial}{\partial\xi}\right)^2 & 0 \end{bmatrix}$$

$$\boldsymbol{B}=\begin{bmatrix} 0 & -1&0&0 \\ -\frac{Ehk}{2(1+\nu)}\left(1+\frac{\partial}{\partial\xi}\right) & 0&0&0 \end{bmatrix} \qquad \boldsymbol{D}=\frac{Ehk}{2(1+\nu)}\begin{bmatrix} 0&0&0&0\\ 0&0&0&0\\ 0&1&0&0\\ 0&0&0&0 \end{bmatrix}$$

$$\boldsymbol{E}=\begin{bmatrix} 0 & 0 \\ 0 & 0 \\ \frac{Ehk}{2(1+\nu)}\left(1+\frac{\partial}{\partial\xi}\right) & 0 \\ 0 & 1 \end{bmatrix} \qquad \boldsymbol{f}_1=q\begin{Bmatrix} 0 \\ \frac{\nu(1+\nu)}{Ehk} \\ \frac{\nu h^2}{10} \\ 0 \end{Bmatrix} \qquad \boldsymbol{f}_2=q\begin{Bmatrix} 0 \\ -1 \end{Bmatrix} \tag{21}$$

Let us now consider a notch formed from several elastic anisotropic materials (Fig. 2). The notch tip is taken as the origin of the cylindrical coordinate system and the notch front as the z-axis. The plate 1 occupies the sectorial domain $[\theta_1, \theta_2]$, named zone 1; the plate 2 occupies the zone 2, bounded by $[\theta_1, \theta_2]$, and so on. Referring to Fig. 2, we adopt the superscript (i) to indicate the quantities in the zone i, for example, $\boldsymbol{v}^{(i)}$, $\boldsymbol{A}^{(i)}$ etc. In each zone, the governing equations have been established in (19), namely:

$$\begin{aligned} \dot{\boldsymbol{v}}_1^{(i)} &= \boldsymbol{A}^{(i)}\boldsymbol{v}_1^{(i)}+\mathrm{e}^{\xi}\boldsymbol{f}_1^{(i)}+\mathrm{e}^{2\xi}\boldsymbol{D}^{(i)}\boldsymbol{v}_1^{(i)}+\mathrm{e}^{2\xi}\boldsymbol{E}^{(i)}\boldsymbol{v}_2^{(i)} \\ \dot{\boldsymbol{v}}_2^{(i)} &= \boldsymbol{B}^{(i)}\boldsymbol{v}_1^{(i)}+\boldsymbol{C}^{(i)}\boldsymbol{v}_2^{(i)}+\mathrm{e}^{\xi}\boldsymbol{f}_2^{(i)} \end{aligned} \tag{22}$$

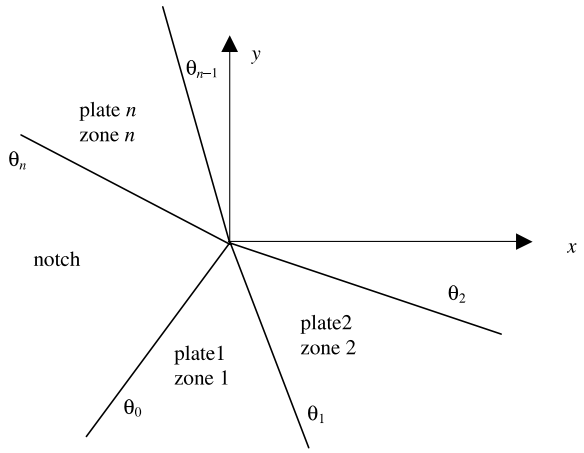

Fig. 2. Notch formed from several anisotropic plates.

Moreover, at the notch tips we have the following boundary conditions:

$$\begin{aligned} &M_{r\theta}(\theta=\theta_0)=M_{\theta\theta}(\theta=\theta_0)=Q_{\theta z}(\theta=\theta_0)=0\\ &M_{r\theta}(\theta=\theta_n)=M_{\theta\theta}(\theta=\theta_n)=Q_{\theta z}(\theta=\theta_n)=0 \end{aligned} \tag{23}$$

According to the definitions in (17), the conditions in (23) are equivalent to:

$$\begin{aligned} &\boldsymbol{p}_1^{(1)}(\theta=\theta_0)=\mathbf{0} \quad \boldsymbol{p}_2^{(1)}(\theta=\theta_0)=\mathbf{0}\\ &\boldsymbol{p}_2^{(n)}(\theta=\theta_n)=\mathbf{0} \quad \boldsymbol{p}_2^{(n)}(\theta=\theta_n)=\mathbf{0} \end{aligned} \tag{24}$$

Across each interface, the displacement components $\{u_r \quad u_\theta \quad w\}$ and the internal forces components $\{M_{r\theta} \quad M_{\theta\theta} \quad Q_{\theta z}\}$ must be continuous. According to (17), these conditions can equivalently be written as follows:

$$\begin{aligned} &\boldsymbol{v}_1^{(1)}(\theta=\theta_1)=\boldsymbol{v}_1^{(2)}(\theta=\theta_1) \qquad \boldsymbol{v}_2^{(1)}(\theta=\theta_1)=\boldsymbol{v}_2^{(2)}(\theta=\theta_1)\\ &\vdots\\ &\boldsymbol{v}_1^{(n-1)}(\theta=\theta_{n-1})=\boldsymbol{v}_1^{(n)}(\theta=\theta_{n-1}) \qquad \boldsymbol{v}_2^{(n-1)}(\theta=\theta_{n-1})=\boldsymbol{v}_2^{(n)}(\theta=\theta_{n-1}) \end{aligned} \tag{25}$$

These relations show the advantage of the choice of the dual variables in the present study: the multi-material problem can be dealt with as a single material problem since the variable vectors $\boldsymbol{v}_1$ and $\boldsymbol{v}_2$ are continuous across all the interfaces. This makes the resolution of the governing equation (19) much easier.

3. Solution method

First, we suppose that the dual variables can be expressed by the following expansion:

$$\boldsymbol{v}_1=\sum_{i=1}^{\infty} \mathrm{e}^{\mu_i\xi}\boldsymbol{\varphi}_i(\theta) \quad \boldsymbol{v}_2=\sum_{i=1}^{\infty} \mathrm{e}^{\lambda_i\xi}\boldsymbol{\psi}_i(\theta) \tag{26}$$

where μ_i, and λ_i are undetermined eigenvalues; $\boldsymbol{\varphi}_i$ and $\boldsymbol{\psi}_i$ are their corresponding eigenvectors depending only on θ. Before resolving (19) with the boundary conditions (24) and the continuity conditions (25), let us

first estimate the smallest eigenvalues and the intervals in which μ and λ lead to singular near-tip fields. Consider now a small region including the crack tip, the strain energy in this region is:

$$U = \frac{1}{2}\int \left[M_{ij}\frac{\tilde{u}_{i,j}+\tilde{u}_{j,i}}{2} + Q_j\left(\tilde{u}_j + w_{,j}\right)\right] \mathrm{d}A \tag{27}$$

$\mathrm{d}A$ being a bidimensional element in the mid-plane. According to the variable changes (6) and (9), $M_{ij} = \widetilde{M}_{ij}/r = \mathrm{O}(r^{\mu_1-1})$, $w = r\tilde{w} = \mathrm{O}(r^{\lambda_1+1})$ when $r \to 0$, we can write therefore:

$$U \approx \int \left[r^{\mu_1-1} r^{\mu_1-1} U_1(\theta) + r^{\lambda_1} r^{\mu_1} U_2(\theta) + r^{\lambda_1} r^{\lambda_1} U_3(\theta)\right] r\,\mathrm{d}\theta\,\mathrm{d}r \tag{28}$$

When $r \to 0$, U must be a finite value, consequently, we have $\mu_1 \geqslant 0$ and $\lambda_1 \geqslant -1$. Moreover, for a singular near-tip field, μ_i and λ_i must be included in the following intervals:

$$0 \leqslant \mu_i < 1 \quad -1 \leqslant \lambda_i < 0 \tag{29}$$

By introducing (26) into (19), we obtain the following eigenvalue problems:

$$\begin{aligned}
&\sum_{i=1}^{\infty}\left(\mathrm{e}^{\mu_i\xi}\dot{\boldsymbol{\varphi}}_i - \boldsymbol{A}_i\mathrm{e}^{\mu_i\xi}\boldsymbol{\varphi}_i\right) = \mathrm{e}^{\xi}\boldsymbol{f}_1 + \sum_{i=1}^{\infty}\left(\mathrm{e}^{2\xi}\boldsymbol{D}_i\mathrm{e}^{\mu_i\xi}\boldsymbol{\varphi}_i + \mathrm{e}^{2\xi}\boldsymbol{E}_i\mathrm{e}^{\lambda_i\xi}\boldsymbol{\psi}_i\right)\\
&\sum_{i=1}^{\infty}\left(\mathrm{e}^{\lambda_i\xi}\dot{\boldsymbol{\psi}}_i - \boldsymbol{C}_i\mathrm{e}^{\lambda_i\xi}\boldsymbol{\psi}_i\right) = \mathrm{e}^{\xi}\boldsymbol{f}_2 + \sum_{i=1}^{\infty}\left(\boldsymbol{B}_i\mathrm{e}^{\mu_i\xi}\boldsymbol{\varphi}_i\right)
\end{aligned} \tag{30}$$

For a single isotropic plate, the matrices $\boldsymbol{A} \sim \boldsymbol{E}$ and the vectors $\boldsymbol{f}_1$ and $\boldsymbol{f}_2$ in (30) are constant quantities. As a consequence, the solutions can be found out under closed form. Some of these solutions are listed in Appendix A.

However, for anisotropic plates, the analytical method to solve the isotropic plate problems cannot directly be used because the quantities $\boldsymbol{A} \sim \boldsymbol{E}$ and the vectors $\boldsymbol{f}_1$ and $\boldsymbol{f}_2$ in (30) are no longer constant. In this work, we present a simple but highly accurate numerical method allowing the determination of the singular near-tip fields.

Now consider the asymptotic near-tip fields by taking $r \to 0$. According to (29) and the relative discussions, the higher order terms can be neglected. As a consequence, we obtain:

$$\dot{\boldsymbol{\varphi}} = \boldsymbol{A}\boldsymbol{\varphi} \quad \dot{\boldsymbol{\psi}} = \boldsymbol{C}\boldsymbol{\psi} \tag{31}$$

with

$$\begin{aligned}
\boldsymbol{A} &= \begin{bmatrix}
\dfrac{s_{41}}{s_{11}}\mu & 1-\mu & \dfrac{12}{h^3}\left(s_{44}-\dfrac{s_{14}^2}{s_{11}}\right) & \dfrac{12}{h^3}\left(s_{42}-\dfrac{s_{41}s_{12}}{s_{11}}\right)\\
\dfrac{s_{12}}{s_{11}}\mu - 1 & 0 & \dfrac{12}{h^3}\left(s_{24}-\dfrac{s_{21}s_{14}}{s_{11}}\right) & \dfrac{12}{h^3}\left(s_{22}-\dfrac{s_{12}^2}{s_{11}}\right)\\
-\dfrac{h^3}{12s_{11}}\mu^2 & 0 & \dfrac{s_{14}}{s_{11}}\mu & \dfrac{s_{12}}{s_{11}}\mu + 1\\
0 & 0 & -1-\mu & 0
\end{bmatrix}\\
\boldsymbol{C} &= \begin{bmatrix}
\dfrac{s_{65}}{s_{55}}(\lambda+1) & \dfrac{1}{hk}\left(s_{66}-\dfrac{s_{56}^2}{s_{55}}\right)\\
-\dfrac{hk}{s_{55}}(1+\lambda)^2 & \dfrac{s_{56}}{s_{55}}(\lambda+1)
\end{bmatrix}
\end{aligned} \tag{32}$$

where μ and λ satisfy (29).

The continuity conditions across the interfaces become:

$$\begin{aligned}
&\boldsymbol{\varphi}^{(1)}(\theta=\theta_1)=\boldsymbol{\varphi}^{(2)}(\theta=\theta_1) \qquad \boldsymbol{\psi}^{(1)}(\theta=\theta_1)=\boldsymbol{\psi}^{(2)}(\theta=\theta_1)\\
&\vdots\\
&\boldsymbol{\varphi}^{(n-1)}(\theta=\theta_{n-1})=\boldsymbol{\varphi}^{(n)}(\theta=\theta_{n-1}) \qquad \boldsymbol{\psi}^{(n-1)}(\theta=\theta_{n-1})=\boldsymbol{\psi}^{(n)}(\theta=\theta_{n-1})
\end{aligned} \tag{33}$$

In order to solve (31), we divide a zone, the zone i bounded by the interface $\theta=\theta_{i-1}$ and $\theta=\theta_i$ for example, into N_i intervals of equal angle size by inserting N_i-1 points. Then we integrate (31) by using the trapezoidal approximation:

$$\begin{aligned}
\boldsymbol{\varphi}_k^{(i)}-\boldsymbol{\varphi}_{k-1}^{(i)}&=\left(\boldsymbol{A}_k^{(i)}\boldsymbol{\varphi}_k^{(i)}+\boldsymbol{A}_{k-1}^{(i)}\boldsymbol{\varphi}_{k-1}^{(i)}\right)\tfrac{d}{2}\\
\boldsymbol{\psi}_k^{(i)}-\boldsymbol{\psi}_{k-1}^{(i)}&=\left(\boldsymbol{C}_k^{(i)}\boldsymbol{\psi}_k^{(i)}+\boldsymbol{C}_{k-1}^{(i)}\boldsymbol{\psi}_{k-1}^{(i)}\right)\tfrac{d}{2}
\end{aligned} \qquad k=1,\ldots,N_i \tag{34}$$

where d is the interval size. From (34), we have:

$$\begin{aligned}
\boldsymbol{\varphi}_k^{(i)}&=\left(\boldsymbol{I}_4-\boldsymbol{A}_k^{(i)}\tfrac{d}{2}\right)^{-1}\left(\boldsymbol{I}_4+\boldsymbol{A}_k^{(i)}\tfrac{d}{2}\right)\boldsymbol{\varphi}_{k-1}^{(i)}\\
\boldsymbol{\psi}_k^{(i)}&=\left(\boldsymbol{I}_2-\boldsymbol{C}_k^{(i)}\tfrac{d}{2}\right)^{-1}\left(\boldsymbol{I}_2+\boldsymbol{C}_k^{(i)}\tfrac{d}{2}\right)\boldsymbol{\psi}_{k-1}^{(i)}
\end{aligned} \quad l \qquad k=1,\ldots,N_i \tag{35}$$

where $\boldsymbol{I}_4$ is a 4×4 unite matrix and $\boldsymbol{I}_2$ is a 2×2 unite matrix. Hence, we immediately obtain the relationship between $\boldsymbol{\varphi}_0^{(i)}(\theta=\theta_{i-1})$ and $\boldsymbol{\varphi}_{N_i}^{(i)}(\theta=\theta_i)$, and that between $\boldsymbol{\psi}_0^{(i)}(\theta=\theta_{i-1})$ and $\boldsymbol{\psi}_{N_i}^{(i)}(\theta=\theta_i)$, namely:

$$\begin{aligned}
\boldsymbol{\varphi}_{N_i}^{(i)}(\theta=\theta_i)&=\boldsymbol{G}^{(i)}\boldsymbol{\varphi}_0^{(i)}(\theta=\theta_{i-1})\\
\boldsymbol{\psi}_{N_i}^{(i)}(\theta=\theta_i)&=\boldsymbol{g}^{(i)}\boldsymbol{\psi}_0^{(i)}(\theta=\theta_{i-1})
\end{aligned} \tag{36}$$

with

$$\begin{aligned}
\boldsymbol{G}^{(i)}&=\left(\boldsymbol{I}_4-\boldsymbol{A}_{N_i}^{(i)}\frac{d}{2}\right)^{-1}\left[\prod_{k=N_i-1}^{1}\left(\boldsymbol{I}_4+\boldsymbol{A}_k^{(i)}\frac{d}{2}\right)\left(\boldsymbol{I}_4-\boldsymbol{A}_k^{(i)}\frac{d}{2}\right)^{-1}\right]\left(\boldsymbol{I}_4+\boldsymbol{A}_0^{(i)}\frac{d}{2}\right)\\
\boldsymbol{g}^{(i)}&=\left(\boldsymbol{I}_2-\boldsymbol{C}_{N_i}^{(i)}\frac{d}{2}\right)^{-1}\left[\prod_{k=N_i-1}^{1}\left(\boldsymbol{I}_2+\boldsymbol{C}_k^{(i)}\frac{d}{2}\right)\left(\boldsymbol{I}_2-\boldsymbol{C}_k^{(i)}\frac{d}{2}\right)^{-1}\right]\left(\boldsymbol{I}_2+\boldsymbol{C}_0^{(i)}\frac{d}{2}\right)
\end{aligned} \tag{37}$$

According to the continuity conditions (33), one has:

$$\boldsymbol{\varphi}_0^{(i)}=\boldsymbol{\varphi}_{N_i}^{(i-1)} \qquad \boldsymbol{\psi}_0^{(i)}=\boldsymbol{\psi}_{N_i}^{(i-1)} \tag{38}$$

Hence, we obtain the relationship between $\boldsymbol{\varphi}^{(1)}(\theta=\theta_n)$ and $\boldsymbol{\varphi}^{(n)}(\theta=\theta_n)$ and that between $\boldsymbol{\psi}^{(1)}(\theta=\theta_0)$ and $\boldsymbol{\psi}^{(n)}(\theta=\theta_n)$, namely:

$$\boldsymbol{\varphi}^{(n)}(\theta=\theta_n)=\boldsymbol{G}\boldsymbol{\varphi}^{(1)}(\theta=\theta_0) \qquad \boldsymbol{\psi}^{(n)}(\theta=\theta_n)=\boldsymbol{g}\boldsymbol{\psi}^{(1)}(\theta=\theta_0) \tag{39}$$

with

$$\boldsymbol{G}=\prod_{i=n}^{1}\boldsymbol{G}^{(i)} \qquad \boldsymbol{g}=\prod_{i=n}^{1}\boldsymbol{g}^{(i)} \tag{40}$$

In practice, the trapezoidal rule provides quite a poor accuracy in calculation of the transfer matrices $\boldsymbol{G}$ and $\boldsymbol{g}$. The accuracy can considerably be improved by using the Richardson extrapolation technique.

Now we write (39) in the form of the dual vectors:

$$\begin{Bmatrix} \boldsymbol{q}_1 \\ \boldsymbol{p}_1 \end{Bmatrix}(\theta=\theta_n) = \begin{bmatrix} \boldsymbol{G}_{11} & \boldsymbol{G}_{12} \\ \boldsymbol{G}_{21} & \boldsymbol{G}_{22} \end{bmatrix} \begin{Bmatrix} \boldsymbol{q}_1 \\ \boldsymbol{p}_1 \end{Bmatrix}(\theta=\theta_0)$$
$$\begin{Bmatrix} \boldsymbol{q}_2 \\ \boldsymbol{p}_2 \end{Bmatrix}(\theta=\theta_n) = \begin{bmatrix} \boldsymbol{g}_{11} & \boldsymbol{g}_{12} \\ \boldsymbol{g}_{21} & \boldsymbol{g}_{22} \end{bmatrix} \begin{Bmatrix} \boldsymbol{q}_2 \\ \boldsymbol{p}_2 \end{Bmatrix}(\theta=\theta_0) \tag{41}$$

Since $\boldsymbol{p}_1(\theta=\theta_0)=\boldsymbol{p}_1(\theta=\theta_n)=\boldsymbol{0}$, and $\boldsymbol{p}_2(\theta=\theta_0)=\boldsymbol{p}_2(\theta=\theta_n)=\boldsymbol{0}$, from (41), one obtains immediately:

$$\boldsymbol{G}_{21}\boldsymbol{q}_1(\theta=\theta_0)=\boldsymbol{0} \qquad \boldsymbol{g}_{21}\boldsymbol{q}_2(\theta=\theta_0)=\boldsymbol{0} \tag{42}$$

These lead to

$$\det|\boldsymbol{G}_{21}(\mu)|=0 \qquad \det|\boldsymbol{g}_{21}(\lambda)|=0 \tag{43}$$

Eq. (43) are the conditions required to determine the eigenvalues μ and λ. Iteration techniques for roots finding can be used for the determination of μ and λ. In this work, the Muller method is used because it can generate complex roots even if a real initial value of μ or λ is chosen, and vice-versa. Theoretically, we can find infinite number of roots from (43). However, only the eigenvalues included in the interval $0\leqslant \mathrm{Re}(\mu)<1$ and $-1\leqslant \mathrm{Re}(\lambda)<0$ are interesting for singular analysis.

Once the eigenvalues determined, the vector $\boldsymbol{q}_1(\theta=\theta_0)$ and $\boldsymbol{q}_2(\theta=\theta_0)$ are obtained from (42). Therefore, the boundary value problem posed becomes an initial value problem. Any numerical method providing a good accuracy can be used for solving Eq. (29). Otherwise the eigenvectors $\boldsymbol{\phi}$ and $\boldsymbol{\psi}$ can straightforwardly be obtained from (35).

4. Numerical examples

In this section, we give some numerical examples showing the accuracy and the possibility of the present method in determining the crack-tip singularities in composite plates.

Example 1: Interfacial crack between two isotropic plates. We suppose that both of the two plates have the same thickness and Poisson coefficient, i.e. $h_1=h_2$, $v_1=v_2=0.3$. By taking different ratios E_1/E_2, we find the following eigenvalues μ and λ which provide singular near-tip fields:

It is seen that the eigenvalues μ are identical to those for corresponding plane stress problems and that the eigenvalues λ are identical to those for corresponding anti-plane problems. In plane stress cases, the imagine part of μ, the oscillatory index ε, can be calculated from the formula $\varepsilon=(2\pi)^{-1}\ln[(1-\beta)/(1+\beta)]$ (Rice, 1988), β being one of the Dundurs parameter (Dundurs, 1969). Comparing with the theoretical formula, all digits in Table 1 are significant.

Example 2: Crack meeting an interface between two mismatched orthotropic plates. We study here a mismatch problem in which the structure is composed by two orthotropic plates, both having the same mechanical properties, but with the material principal axes in different directions. In this example, we use the following compliance matrix:

Table 1
Eigenvalues for an interfacial crack between two isotropic plates

E_1/E_2	2	3	5	10
μ	$0.5\pm0.037306i$	$0.5\pm0.056284i$	$0.5\pm0.075666i$	$0.5\pm0.093774i$
λ	−0.5	−0.5	−0.5	−0.5

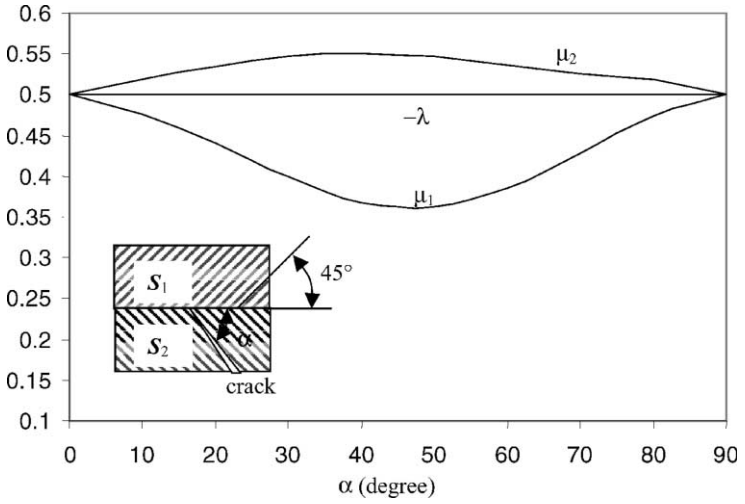

Fig. 3. Singularities for a crack meeting an interface between two mismatched orthotropic plates.

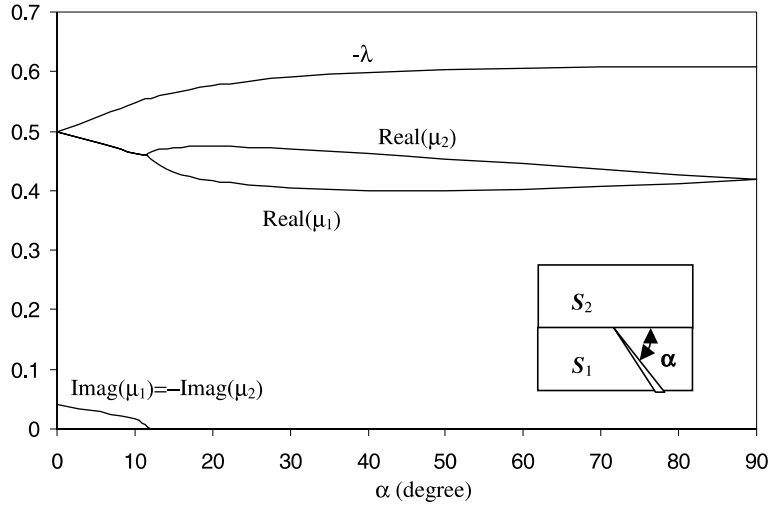

Fig. 4. Singularities for a crack meeting an interface between two orthotropic plates, crack in stiffer plate.

$$\boldsymbol{S} = \begin{bmatrix} 1/39 & -0.0451/6.4 & -0.3507/30.6 & 0 & 0 & 0 \\ & 1/6.4 & -0.275/30.6 & 0 & 0 & 0 \\ & & 1/30.6 & 0 & 0 & 0 \\ & & & 1/4.5 & 0 & 0 \\ & \text{Sym.} & & & 1/19.7 & 0 \\ & & & & & 1/4.5 \end{bmatrix} \tag{44}$$

The plate 1 is subjected to a 45° rotation around the z-axis, while the plate 2 is subjected to a −45° rotation around the z-axis. We suppose that the crack lies in plate 2 with an inclined angle α with respect to the interface. For different α, the eigenvalues leading to singular fields are plotted in Fig. 3.

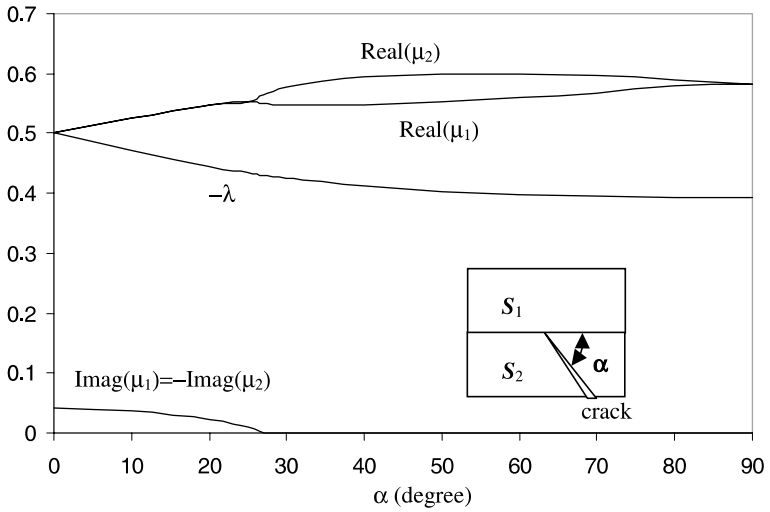

Fig. 5. Singularities for a crack meeting an interface between two orthotropic plates, crack in the less stiffer plate.

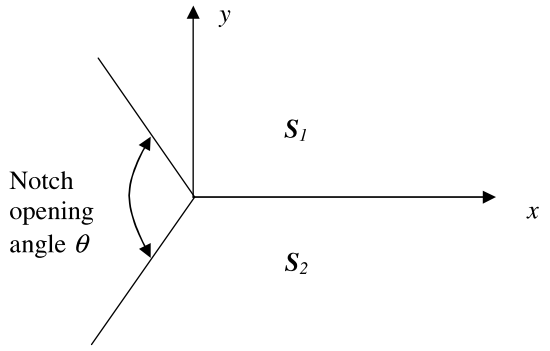

Fig. 6. A notch symmetrically formed from two orthotropic plates.

Table 2
Singularities near the notch-tip formed from two orthotropic plates

Notch angle	μ_1	μ_2	λ
0°	$0.5 + 0.0412294i$	$0.5 - 0.0412294i$	−0.5
60°	0.5450832	0.8646145	−0.3056547
120°	0.6812632	1	−0.1463226
180°	0.9886141	1	0
240°	1	1.79255	0.2068588

Fig. 3 shows that the eigenvalue λ is not influenced by the crack incident angle, while the two eigenvalues μ_1 and μ_2 are different from $1/2$, one weaker and another stronger, when α is different from 0° or from 90°.

Example 3: Crack meeting an interface between two orthotropic plates. Now suppose that we have two orthotropic plates bonded together but with one stiffer than another. In this example, the compliance matrix of plate 1, the stiffer one, is taken as $\boldsymbol{S}_1 = \boldsymbol{S}$, $\boldsymbol{S}$ being given in (44), and the compliance matrix of plate 2, the less stiff plate, is taken as $\boldsymbol{S}_2 = 2\boldsymbol{S}_1$. Let the crack be situated first in plate 1, then in plate 2. The

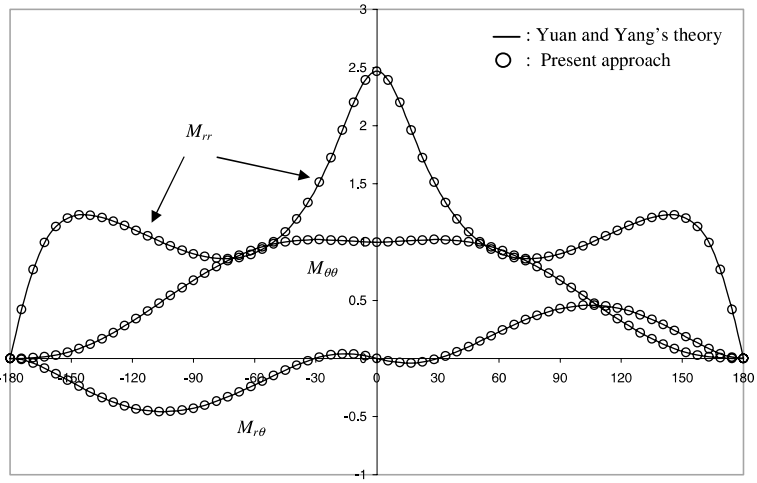

Fig. 7. Angular variations of the bending moments in an orthotropic plate, symmetrical near-tip field.

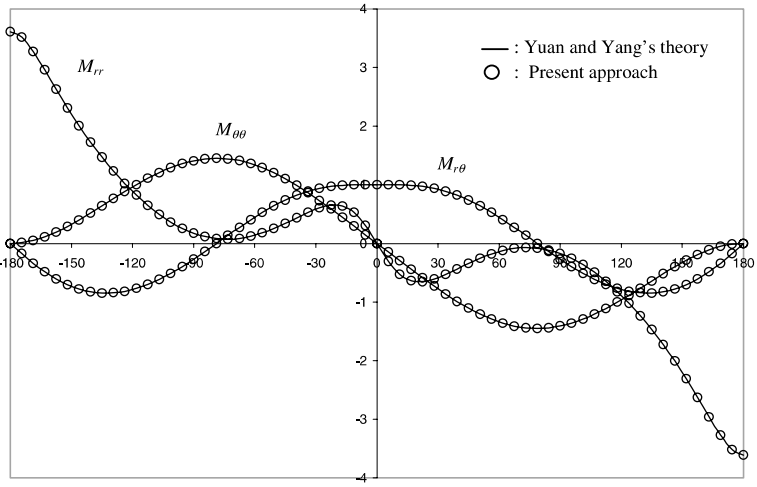

Fig. 8. Angular variations of the bending moments in an orthotropic plate, anti-symmetrical near-tip field.

eigenvalues leading to singular fields are computed for different crack incident angles and plotted in Figs. 4 and 5. In both cases, one can observe the oscillationary nature for small crack incident angle with respect to the interface. When the crack lies in the less stiff (stiffer) plate, weak (strong) singularities are obtained. These properties are similar to those observed in the corresponding plane problems (Li et al., 1997, 2001).

Example 4: Notch formed by two orthotropic plates. Consider a notch formed symmetrically from two orthotropic plates (Fig. 6). Same material properties are used as in the precedent example, i.e., $\boldsymbol{S}_1 = \boldsymbol{S}$, $\boldsymbol{S}$ being given in (44), $\boldsymbol{S}_2 = 2\boldsymbol{S}_1$. The first three eigenvalues are evaluated and listed in Table 2 for different notch opening angles. It is seen that the stress singularities decrease as the notch opening angle increases. It is also interesting to observe that the stress singularities may exist even for a 180° notch.

Example 5: Crack in an orthotropic plate. Let us consider a crack in a single orthotropic plate and evaluate the leading order field near the crack tip. This problem has been solved by Yuan and Yang (2000)

using the Stroh formalism. It can naturally be solved by using the present approach. The compliance matrix used in this example is given in (44). Figs. 7 and 8 illustrate the comparison between the angular variations of the bending moments computed from both the approaches. It can be seen that the two approaches provide exactly the same results. It is to note that the present approach does not present any degeneration problem, it can be used in isotropic problems as well as in anisotropic ones.

5. Concluding remarks

In this work, we have developed a new approach to analyze the near-tip fields of through-the-thickness cracks in thin plates subjected to bending. The Reissner plate theory is used in the present approach. By establishing dual differential equations in the frame of the Hamiltonian system, a large range of problems in this topic, some of them are somewhat difficult to treat with the traditional techniques, can be solved in rather a simple way.

Appendix A

For a single isotropic plate with a semi-infinite crack, the asymptotic fields near the crack tip can be written in closed form. The present approach permits to find out the solutions more easily comparing to the traditionally used methods.

The governing differential equation (30) can be resolved by recurrence. First, we seek the solutions for $i = 1$ and 2 which need only to resolve the homogeneous differential equations. Then we increase successively i and some non-homogeneous differential equations are obtained. The non-homogeneous terms are already known from lower order solutions. Thus we can find successively all eigenvalues and eigenvectors in expansions (26).

A.1. Solutions for i = 1 and 2

Consider the smallest eigenvalues (29). We can neglect the right-hand-side terms in (30), because, when $r \to 0$, $\xi \to -\infty$ these terms tend to zero comparing those in the left hand side. We have therefore:

$$\dot{\boldsymbol{\varphi}}_i = \boldsymbol{A}_i \boldsymbol{\varphi}_i \quad i = 1, 2 \tag{A.1}$$

$$\dot{\boldsymbol{\psi}}_i = \boldsymbol{C}_i \boldsymbol{\psi}_i \quad i = 1, 2 \tag{A.2}$$

with

$$\boldsymbol{A}_i = \begin{bmatrix} 0 & 1-\mu_i & \dfrac{24(1+v)}{Eh^3} & 0 \\ -1-v\mu_i & 0 & 0 & \dfrac{12(1-v^2)}{Eh^3} \\ -\dfrac{Eh^3}{12}\mu_i^2 & 0 & 0 & 1-v\mu_i \\ 0 & 0 & -1-\mu_i & 0 \end{bmatrix} \quad i = 1, 2$$

$$\boldsymbol{C}_i = \begin{bmatrix} 0 & \dfrac{2(1+v)}{Ehk} \\ -\dfrac{Ehk}{2(1+v)}(1+\lambda_i)^2 & 0 \end{bmatrix} \tag{A.3}$$

The solutions of the homogeneous differential equation systems (A.1) and (A.2) are easy to found out. By performing a standard eigenfunction analysis, we can easily obtain:

$$\begin{aligned}&\mu = n/2\\&\lambda = n/2 - 1\end{aligned}\qquad n = 0, 1, 2, \ldots \tag{A.4}$$

Here the eigenvalues $\mu < 0$ and $\lambda = -1$ are omitted according to Eq. (29).

The general solutions of (A.1) and (A.2) are:

$$\begin{aligned}\boldsymbol{\varphi}_i^{(g)} = &\begin{Bmatrix} -a_i \dfrac{1}{D\mu}\cos(1+\mu_i)\theta + c_i \dfrac{\chi-\mu_i}{D\mu_i(1+\mu_i)}\cos(1-\mu_i)\theta \\ a_i \dfrac{1}{D\mu_i}\sin(1+\mu_i)\theta - c_i \dfrac{\chi+\mu_i}{D\mu_i(1+\mu_i)}\sin(1-\mu_i)\theta \\ a_i \sin(1+\mu_i)\theta + c_i \dfrac{1-\mu_i}{1+\mu_i}\sin(1-\mu_i)\theta \\ a_i \cos(1+\mu_i)\theta + c_i \cos(1-\mu_i)\theta \end{Bmatrix}\\ &+ \begin{Bmatrix} -b_i \dfrac{1}{D\mu_i}\sin(1+\mu_i)\theta + d_i \dfrac{\chi-\mu_i}{D\mu_i(1+\mu_i)}\sin(1-\mu_i)\theta \\ -b_i \dfrac{1}{D\mu_i}\cos(1+\mu_i)\theta + d_i \dfrac{\chi+\mu_i}{D\mu_i(1+\mu_i)}\cos(1-\mu_i)\theta \\ -b_i \cos(1+\mu_i)\theta - d_i \dfrac{1-\mu_i}{1+\mu_i}\cos(1-\mu_i)\theta \\ b_i \sin(1+\mu_i)\theta + d_i \sin(1-\mu_i)\theta \end{Bmatrix}\end{aligned} \tag{A.5}$$

$$\boldsymbol{\psi}_i^{(g)} = \begin{Bmatrix} \dfrac{1+\lambda_i}{G}[e_i \cos(1+\lambda_i)\theta + f_i \sin(1+\lambda_i)\theta] \\ e_i \cos(1+\lambda_i)\theta - f_i \sin(1+\lambda_i)\theta \end{Bmatrix} \tag{A.6}$$

with $\chi = (3-\nu)/(1+\nu)$, $G = E/(2(1+\nu))$ and $D = (Eh^3)/(12(1+\nu))$. $a_i, \ldots, f_i$ are constant coefficients and satisfy the following relationships:

$$\begin{aligned}&(1+\mu_i)a_i = (1-\mu_i)c_i \quad b_i = d_i \quad \text{if } \mu_i = 1/2, 3/2 \ldots\\&a_i = -c_i \quad (1+\mu_i)b_i = -(1-\mu)d_i \quad \text{if } \mu_i = 0, 1, 2 \ldots\end{aligned} \tag{A.7}$$

and

$$\begin{aligned}&e_i = 0 \quad \text{if } \lambda_i = -1/2, 1/2 \cdots\\&f_i = 0 \quad \text{if } \lambda_i = -1, 0, 1 \cdots\end{aligned} \tag{A.8}$$

The eigenvalues $\mu_1 = 0$ and $\lambda_1 = -1$ correspond to some rigid motions of the plate. With the eigenvalues $\mu_2 = 1/2$ and $\lambda_2 = -1/2$, we obtain the singular near-tip field. Return to conventional notations, we have:

$$\begin{aligned}u_r &= \frac{K_1 z}{2D}\sqrt{\frac{r}{2\pi}}\left[-\cos\frac{3\theta}{2} + (2\chi-1)\cos\frac{\theta}{2}\right] + \frac{K_2 z}{2D}\sqrt{\frac{r}{2\pi}}\left[3\sin\frac{3\theta}{2} - (2\chi-1)\sin\frac{\theta}{2}\right]\\ u_\theta &= \frac{K_1 z}{2D}\sqrt{\frac{r}{2\pi}}\left[\sin\frac{3\theta}{2} - (2\chi+1)\sin\frac{\theta}{2}\right] + \frac{K_2 z}{2D}\sqrt{\frac{r}{2\pi}}\left[3\cos\frac{3\theta}{2} - (2\chi+1)\cos\frac{\theta}{2}\right]\\ w &= \frac{1+\nu}{Ehk}\sqrt{\frac{r}{2\pi}}K_3 \sin\frac{\theta}{2}\end{aligned} \tag{A.9}$$

and

$$
\begin{aligned}
M_{rr} &= \frac{K_1}{4\sqrt{2\pi r}}\left[-\cos\frac{3\theta}{2}+5\cos\frac{\theta}{2}\right]+\frac{K_2}{4\sqrt{2\pi r}}\left[3\sin\frac{3\theta}{2}-5\sin\frac{\theta}{2}\right]\\
M_{\theta\theta} &= \frac{K_1}{4\sqrt{2\pi r}}\left[\cos\frac{3\theta}{2}+3\cos\frac{\theta}{2}\right]+\frac{K_2}{4\sqrt{2\pi r}}\left[-3\sin\frac{3\theta}{2}-3\sin\frac{\theta}{2}\right]\\
M_{r\theta} &= \frac{K_1}{4\sqrt{2\pi r}}\left[\sin\frac{3\theta}{2}+\sin\frac{\theta}{2}\right]+\frac{K_2}{4\sqrt{2\pi r}}\left[3\cos\frac{3\theta}{2}+\cos\frac{\theta}{2}\right]\\
Q_{rz} &= \frac{K_3}{\sqrt{2\pi r}}\sin\frac{\theta}{2}\\
Q_{\theta z} &= \frac{K_3}{\sqrt{2\pi r}}\cos\frac{\theta}{2}
\end{aligned}
\tag{A.10}
$$

The constants K_1 and K_2 are similar to the stress intensity factors in plane crack problems while K_3 is similar to the stress intensity factor K_{III} for anti-plane deformation cracks. These results are identical to those obtained by Hartranft and Sih (1968), using the Reissner plate theory and the integral transformation technique. Here we obtain them by using elementary mathematical tools.

A.2. Solutions for $i > 2$

Knowing the values of μ_i, λ_i and the solutions for $i = 1$ and 2, we can seek the higher orders solutions for $i > 2$. By gathering the terms of the same order in (30), we obtain the following recurrence equations:

$$
\begin{aligned}
&\dot{\boldsymbol{\varphi}}_3 - \boldsymbol{A}_3\boldsymbol{\varphi}_3 = \boldsymbol{f}_1 + \boldsymbol{E}_1\boldsymbol{\psi}_1\\
&\dot{\boldsymbol{\varphi}}_4 - \boldsymbol{A}_4\boldsymbol{\varphi}_4 = \boldsymbol{E}_2\boldsymbol{\psi}_2\\
&\dot{\boldsymbol{\varphi}}_i - \boldsymbol{A}_i\boldsymbol{\varphi}_i = \boldsymbol{E}_{i-2}\boldsymbol{\psi}_{i-2} + \boldsymbol{D}_{i-4}\boldsymbol{\varphi}_{i-4} \quad i \geqslant 5
\end{aligned}
\tag{A.11}
$$

and

$$
\begin{aligned}
&\dot{\boldsymbol{\psi}}_3 - \boldsymbol{C}_3\boldsymbol{\psi}_3 = \boldsymbol{f}_2 + \boldsymbol{B}_1\boldsymbol{\varphi}_1\\
&\dot{\boldsymbol{\psi}}_i - \boldsymbol{C}_i\boldsymbol{\psi}_i = \boldsymbol{B}_{i-2}\boldsymbol{\varphi}_{i-2} \quad i \geqslant 4
\end{aligned}
\tag{A.12}
$$

(A.11) and (A.12) are non-homogeneous differential equation systems. Their solutions include two parts: the general ones and the particular ones. The general solutions have been given in (A.5) and (A.6). The particular solutions for $i \geqslant 3$ can be found out successively by considering the right hand terms in (A.11) and (A.12) already known from lower order solutions. We list here only the particular solutions for $i = 3$ and 4.

(1) for $i = 3$:

$$
\begin{aligned}
&\boldsymbol{\varphi}_3^{(p)}(\mu_3 = 1) = \left\{-\tfrac{qv}{Ehk} \quad 0 \quad 0 \quad 0\right\}^{\mathrm{T}}\\
&\boldsymbol{\psi}_3^{(p)}(\lambda_3 = 0) = \left\{-\tfrac{1}{G}q \quad 0\right\}^{\mathrm{T}}
\end{aligned}
\tag{A.13}
$$

(4) for $i = 4$:

$$\boldsymbol{\varphi}_4^{(p)}(\mu_4 = 3/2) = f_2 \begin{Bmatrix} \dfrac{4}{3(1+v)h^2}\sin\dfrac{\theta}{2} \\ \dfrac{4(2+3v)}{3(1+v)h^2}\cos\dfrac{\theta}{2} \\ \dfrac{Ehk}{12(1+v)}\cos\dfrac{\theta}{2} \\ 0 \end{Bmatrix}$$

$$\boldsymbol{\psi}_4^{(p)}(\lambda_4 = 1/2) = a_2 \begin{Bmatrix} \frac{1}{D}\left[\dfrac{4(7+v)}{3(1+v)}\cos\dfrac{3\theta}{2} - \dfrac{4(1-v)}{1+v}\cos\dfrac{\theta}{2}\right] \\ \dfrac{-120}{h^2(1+v)}\left[\sin\dfrac{3\theta}{2} + \sin\dfrac{\theta}{2}\right] \end{Bmatrix} + b_2 \begin{Bmatrix} \dfrac{4(1-v)}{D(1+v)}\sin\dfrac{\theta}{2} \\ \dfrac{60}{h^2}\left[\cos\dfrac{3\theta}{2} - \dfrac{2}{1+v}\cos\dfrac{\theta}{2}\right] \end{Bmatrix} \tag{A.14}$$

It is to note that the results listed in this appendix are identical to those found in previous works, using displacement eigenfunction method (Sosa and Eischen, 1986, Su and Leung, 2001) or using Stroh formalism (Yuan and Yang, 2000). One of the advantages of the present method is that the displacement and internal force components are obtained simultaneously.

References

Ang, D.D., Williams, M.L., 1961. Combined stresses in a orthotropic plate having a finite crack. ASME Journal of Applied Mechanics 28, 372–378.

Boduroglu, H., Erdogan, F., 1983. Internal and edge cracks in a plate of finite width under bending. Journal of Applied Mechanics 50, 621–629.

Delale, F., Erdogan, F., 1979. The effect of transverse shear in a crack plate under skew-symmetric loading. Journal of Applied Mechanics 46, 618–624.

Dundurs, J., 1969. Edge-bonded dissimilar orthogonal elastic wedges. ASME Journal of Applied Mechanics 29, 650–652.

Hartranft, R.J., Sih, G.C., 1968. Effect of plate thickness on the bending stress distribution around through cracks. Journal of Mathematics and Physics 47, 276–291.

Hui, C.Y., Zehnder, A.T., 1993. A theory for fracture of thin plates subjected to bending and twisting moments. International Journal of Fracture 61, 211–229.

Knowels, J.K., Wang, N.W., 1960. On the bending of an elastic plate containing a crack. Journal of Mathematics and Physics 39, 223–236.

Murthy, M.V.V., Raju, K.N., Viswanath, S., 1981. On the bending stress distribution at the tip of a stationary crack from Reissner's theory. International Journal of Fracture 17, 537–552.

Li, J., Zhang, X.B., Recho, N., 1997. Investigation of an arbitrarily oriented crack meeting an interface between two elastic materials. European Journal of Mechanics A/Solid 16 (5), 795–821.

Li, J., Zhang, X.B., Recho, N., 2001. Stress singularities near the tip of a two-dimensional notch formed from several elastic anisotropic materials. International Journal of Fracture 107, 379–395.

Rice, J.R., 1988. Elastic fracture mechanics concepts for interfacial cracks. ASME Journal of Applied Mechanics 55, 98–103.

Sih, G.C., 1962. Flexural problems of cracks in mixed media. In: Proceedings of the First International Conference on Fracture, vol. 1, pp. 391–409.

Sih, G.C., Chen, E.P., 1981. Cracks in composite materials. In: Mechanics of Fracture, vol. 6. Martinus Nijhoff Publishers, The Hague.

Sih, G.C., Rice, J.R., 1964. The bending of plates of dissimilar media. Journal of Applied Mechanics 31, 477–482.

Sih, G.C., Paris, P.C., Erdogan, F., 1962. Crack tip stress intensity factors for plane extension and plate bending problems. Journal of Applied Mechanics 48, 320–326.

Sosa, H.A., Eischen, J.W., 1986. Computation of stress intensity factors for plate bending via a path-independent integral. Engineering Fracture Mechanics 25, 451–462.

Su, R.K.L., Leung, A.Y.T., 2001. Mixed mode crack in Reissner plates. International Journal of Fracture 107, 235–257.
Williams, M.L., 1961. The bending stress distribution at the base of a stationary crack. Journal of Applied Mechanics 28, 78–82.
Young, M.L., Sun, C.T., 1993. Cracked plates subjected to out-of-plane tearing loads. International Journal of Fracture 60, 1–18.
Yuan, F.G., Yang, S., 2000. Asymptotic crack-tip fields in an anisotropic plate subjected to bending, twisting moments and transverse shear loads. Composites Science and Technology 60, 2489–2502.
Zhong, W.X., 1995. A systematic methodology for theory of elasticity. Dalian University of Technology Press.